17

Stress-Induced Phase Transitions in Metallocene-Made Isotactic Polypropylene

Claudio De Rosa, Finizia Auriemma

Dipartimento di Chimica, Università di Napoli "Federico II", Complesso Monte S.Angelo, Via Cintia, 80126 Napoli, Italy
claudio.derosa@unina.it

Abstract. The deformation behavior of semicrystalline polymers associated with polymorphic transformations under tensile deformation is discussed in the case of isotactic polypropylene (iPP). The mechanical properties and polymorphic transformations occurring during plastic deformation of iPP samples with variable stereoregularity, containing only *rr* stereo-defects, are presented. Thermoplastic materials showing high stiffness, or high flexibility, or elastic properties can be produced depending on the concentration of defects. We report a phase diagram of iPP where the regions of stability of the different polymorphic forms are defined as a function of the degree of stereoregularity and deformation. The values of critical strain corresponding to the structural transformations depend on the stereoregularity that affects the relative stability of the involved polymorphic forms and the state of the entangled amorphous phase. In the case of elastomeric iPP, we show that samples of different stereoregularity present different types of elasticity depending on the degree of crystallinity. The more stereoregular samples, with *rr* content in the range 7–11% show elastic behavior in spite of the high degree of crystallinity (40–50%). Since elasticity is generally a property of the amorphous phase, probably elasticity in these samples is partially due to the enthalpic contribution associated with the crystallization of the mesomorphic form into the α-form occurring upon releasing the tension. In the case of the less stereoregular sample, with *rr* content of $\approx$17%, the degree of crystallinity is very low, and elasticity has essentially entropic origin, as in conventional elastomers.

17.1 Introduction

Semicrystalline polymers consist of two phases, crystalline and amorphous. The morphology that develops in polymers upon crystallization from the melt may be described in terms of lamellar crystals alternating to amorphous regions, forming a highly entangled network. The lamellar crystals usually have thickness of order of some ten nanometers, whereas the lateral dimensions are much larger. Since the polymer chains in the crystalline phase are oriented perpendicular to the lateral dimensions of the lamellae and the length of the

C. De Rosa and F. Auriemma: *Stress-Induced Phase Transitions in Metallocene-Made Isotactic Polypropylene*, Lect. Notes Phys. **714**, 345–371 (2007)
DOI 10.1007/3-540-47307-6_17

chains is much larger than the lamellar thickness, each chain may run through several crystalline and amorphous regions. Connections between neighboring crystals are thus ensured by chains emanating from one lamella that enter the other and by entanglements involving chains that re-enter into the same crystalline lamella, after passage through a portion of the adjoining amorphous layer [1].

This complex morphology entails that large, irreversible deformations may occur by cold drawing semicrystalline polymers at a temperature higher than the glass transition temperature. During stretching, indeed, the initial isotropic structure, characterized by the random orientation of the polymer segments in the amorphous and crystalline regions, is gradually transformed into a fiber morphology, i.e. highly anisotropic structure, characterized by preferential orientation of the macromolecular chains along the stretching directions [2]. The development of a fibrous morphology starting from the spherulitic structure is an irreversible process, the original spherulitic morphology can be re-obtained only by melting of the fibrous material and successive recrystallization. Therefore, the stretching of crystalline polymers inevitably involves large plastic (irreversible) deformations.

The mechanisms of plastic deformation at microscopic level of amorphous polymers are mainly crazing and shear yielding [3–5]. In semicrystalline polymers, although the glass transition temperature, density, infrared spectrum and other properties of the amorphous phase interdispersed between the crystalline lamellae are close to those of bulk amorphous polymers, the mechanisms of plastic deformation are very different from those of the amorphous materials, since also the crystalline phase plays a key role [1]. However, because of the presence of the entangled amorphous phase, the mechanisms of plastic deformation of semicrystalline polymers are also different from those of other crystalline materials (for instance metals).

The mechanism of plastic deformation in polymers is rather complicated and involves different phenomena, which occur on the same time scale of applied stress and on different length scales. The global deformation behavior of semicrystalline polymers at temperatures higher than the glass transition temperature may be regarded as the stretching of two interpenetrated networks, made by the interlocked crystalline lamellae and the entangled amorphous phase, characterized by a large nonlinerar internal viscosity [6]. Deformation is accompanied by slip processes within the lamellae, and intralamellar mosaic block slips, and, at larger strain, when the stress acting on the crystallites reaches a value at which the crystalline blocks are no longer stable, by stress-induced melting and recrystallization in new oriented crystallites, whose assembly forms fibrils [6]. The principal modes of deformation on the crystallographic length scale may be slips, twinnings, [2, 6] martensitic transformations, [7] stress-induced melting [8] and recrystallization, [1] and formation of nanoblocks in the amorphous phase [9]. Collective intra-lamellar slip processes, collective motions of lamellar stacks [2,3,6] and formation of microvoids [3,7,9] may occur at a larger length scale. Furthermore, transient phenomena may

also be involved. For instance, orientation of portion of crystalline lamellae with the chain axes nearly perpendicular to the stretching direction may occur at low deformations, that is, after the initial Hooke's elastic range, close to the yield point, and disappears at higher deformations [6, 10].

The stress-strain behavior of polymeric materials depends on the properties of the material, including molecular weight, polydispersity, the microstructure of the chains (i.e. concentration and distribution of stereodefects and regiodefects, constitutional defects as typically the presence of comonomeric units), packing, chain entanglements, crystallinity, heterogeneity, defects in the crystals (e.g. dislocations, point defects, structural disorder), and several other parameters as temperature, pressure, load rate, the shape of the item under load, etc. At variance with cross-linked amorphous polymer networks, that show large reversible deformations and positive temperature coefficients of stress, semicrystalline polymers generally exhibit negative stress-temperature coefficients and only short-range elasticity when stretched samples are relaxed by releasing the tensile stress.

According to a generalized view the mechanisms that govern the process of tensile deformation of semicrystalline polymers at low and moderate deformations appears to be strain-controlled, rather than stress-controlled [6, 10–13]. This may be evidenced by the fact that along the true stress-strain curves of several polymeric materials different regimes are discernible, corresponding to changes in the differential compliance that take place at defined critical points [6, 10–13]. These critical points have been interpreted as i) the onset of isolated inter and intra-lamellar slip processes after the initial Hooke's elastic range (point A); ii) change into a collective activity of slip motions of crystal blocks at the point of maximum curvature of the true stress-strain curve (point B); iii) the beginning of destruction of crystal blocks followed by re-crystallization with formation of fibrils (point C) and iv) the beginning of disentanglement of the amorphous network or strain hardening due to the stretching of the amorphous entangled network at high deformations (point D).

The values of the strains at critical points A, B and C are constant, for each class of polymer, when varying crystallinity, temperature, strain rate and crystal thickness [6, 10–13]. Opposite to the strain, the stresses at critical points vary, with larger values for higher crystallinities and lower values for higher temperatures. The observation complies with the general assumption that in semicrystalline polymers (and in heterogeneous systems in general e.g. composite materials) whereas the stress is not homogeneously distributed, the strain, instead, is homogeneously distributed [3,6,14]. At low stresses or strains the forces transmitted by the interconnected crystallites dominate, whereas at high strains the rubber-like network forces are superior [14].

The yield point in engineering stretching experiments is always located shortly above point B. The position of the critical strain at the point C, at which the critical stress that starts destructing the crystal blocks is achieved, depends on the interplay between the entanglement density of the amorphous

phase and the intrinsic stability of crystals [6]. A higher entanglement density implies a higher stress that is generated when the sample is stretched. The more stable the crystallites, the higher the stress needed for their destruction [6].

The role of cavitation versus plastic deformation of crystals during stretching of crystalline polymers has been recently studied by Galeski [15]. Cavitation corresponds to formation of microvoids in the amorphous layers confined between crystalline lamellae. During stretching of semicrystalline polymers there is a competition between cavitation and activation of crystal plasticity: easiest phenomena occur first, that is cavitation in polymers with crystals of higher plastic resistance, and plastic deformation of crystals in polymers with crystals of lower plastic resistance. The stress level at yield point corresponds to the onset of cavitation and not necessarily to the onset of plastic deformation of crystals. In polymers where cavitation is preponderant over the plastic deformation of crystals, low strain hardening and intense chain disentanglement take place during drawing at high draw ratio [15]. Strain hardening and no significant disentanglement takes place, instead, during plastic deformation of polymers up to high strains, provided that there is no cavitation [15]. Cavitation is negligible either for polymers having crystals with low plastic resistance or for polymers having crystals with high plastic resistance subjected to cavity-free deformation as for instance plane strain compression in a channel die [15].

This complex picture may be further complicated by occurrence of polymorphic transformations during plastic deformation at large degrees of deformation, that is, after the yield point. In fact, in many polymers the crystalline form that develops upon stretching may be different from the stable form present in the melt-crystallized undeformed samples. Moreover, in some cases, stretching may cause the disruption of lamellar crystals through the pulling out of chains from the crystals, leading to the formation of a mesophase, i.e. a solid phase characterized by large amount of structural disorder that may be considered as intermediate between amorphous and crystalline phases [16]. When the crystalline form that develops by stretching is metastable, it may transform back into the more stable form previously present in the unoriented sample, or into another polymorphic form, by removing the tensile stress. In some highly crystalline polymers the polymorphic transition occurring upon releasing the tension is reversible and is associated with a non trivial recovery of the initial dimensions of the sample (long range elasticity) [17–21]. The entity of plastic versus elastic deformation experienced by the material upon releasing the stress, may critically depend on the relative stabilities of the two crystalline phases that develop during successive cycles of stretching and relaxation. The enthalpic gain of the reversible crystal-crystal phase transition occurring upon releasing the tension may play a key role in the elasticity of these materials [20, 21].

The non-trivial role of the crystalline phase in the deformation behavior of semicrystalline polymers is here illustrated in the case metallocene-made isotactic polypropylene (iPP).

The development of single center catalysts for the polymerization of olefins has allowed production of new materials having microstructures that cannot be obtained with conventional Ziegler-Natta catalysts [22–25]. In the case of polypropylene, samples with any type and degree of stereoregularity, from highly isotactic to highly syndiotactic polypropylene can be produced [25]. The fine-tuning of the microstructure is nowadays possible through the rational choice of the catalytic system, and polypropylenes characterized by different kinds and amounts of regio- and stereo-irregularities, different distributions of defects, and different molecular weights, are now available [25]. The mechanical properties of these polymers depend on the crystallization behavior, which, in turn, depends on the chain microstructure and, in particular, on the stereoregularity [17–21].

The mechanical properties and the polymorphic transitions occurring during stretching of metallocene-made iPP samples with different amounts of stereo-irregularities (mainly isolated *rr* triads) are here discussed. Depending on stereoregularity, thermoplastic materials showing high stiffness, or high flexibility, or elastic properties can be produced [17, 18]. We show that different polymorphic transitions are involved during stretching of these samples [17, 18] and that stress-induced phase transitions are strain controlled rather than stress controlled [26]. A phase diagram of iPP is built up where the regions of stability of the different polymorphic forms of iPP are defined as a function of stereoregularity and degree of deformation. Finally we show that the elastic behavior of less crystalline and stereoregular samples is associated with a reversible polymorphic transition and that elastomeric iPP samples present rubber-like elasticity which originates from different mechanisms, depending on the degree of crystallinity.

17.2 Mechanical Properties of Unoriented Films

Samples of iPP of different stereoregularity containing only one kind of stereodefect (isolated *rr* triads), with variable concentration in a wide range and uniformly distributed along the chains, and containing no measurable amount of regioerrors, have been prepared with the different metallocene catalysts of Fig. 17.1, activated with methylalumoxane (MAO) [27–31]. The amount of *rr* defects depend on the structure of the catalyst, in particular the indenyl substituents, and the conditions of polymerization, and can be varied in the range between 0.5 and 17% [17,18]. Correspondingly the samples show melting temperatures variable between 162 and 45°C (Table 17.1) [17, 18].

Samples used for the study of the structural transformations occurring during stretching and for the mechanical tests have been prepared by compression molding. The X-ray powder diffraction profiles of melt-crystallized

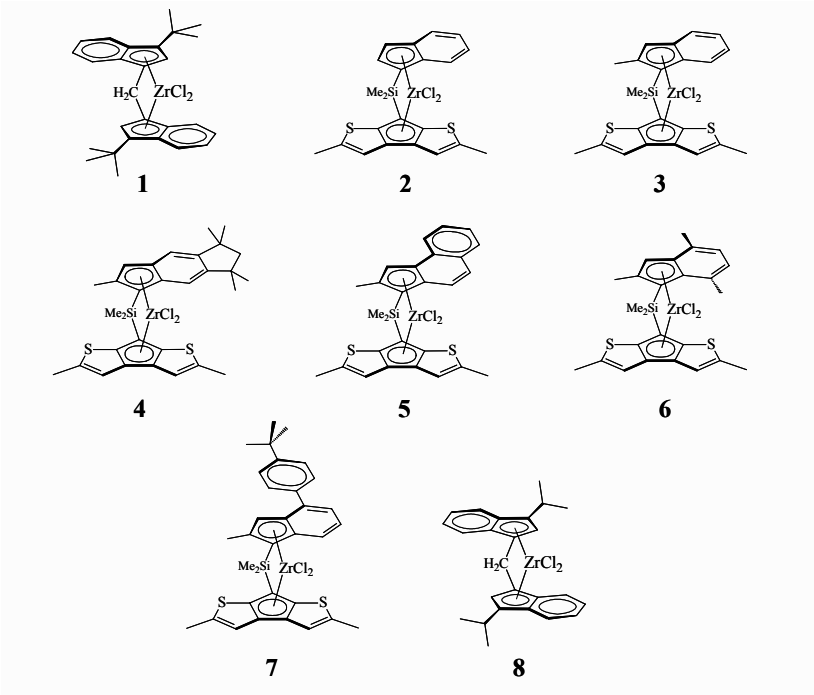

Fig. 17.1. Structure of C_2-symmetric (**1,8**) and C_1-symmetric (**2**–**7**) pre-catalysts

Table 17.1. Molecular masses (M_v), melting temperatures (T_m) and content of *rr* triad and *mmmm* pentad stereosequences of iPP samples prepared with catalysts of Chart 1[a]

Sample	catalyst/cocatalyst	M_v^b	T_m (°C)[c]	*mm* %	*mr* %	*rr* %	*mmmm* %
iPP1	1/MAO	195,700	162	98.5	1.0	0.49	97.5
iPP2	7/MAO	106,000	140	92.4	5.1	2.54	87.6
iPP3	6/MAO	202,400	133	88.9	7.4	3.70	82.2
iPP4	3/MAO	505,800	119	83.4	11	5.52	73.9
iPP5	5/MAO	210,900	116	82.2	11.8	5.92	72.2
iPP6	2/MAO	166,400	111	76.9	15.4	7.68	64.5
iPP7	4/MAO	123,400	84	66.9	22.0	11.01	51.0
iamPP[d]	8/MAO	143,700	45	54.0	28.9	17.1	35

[a] No or negligible regioerrors (2,1 insertions) could be observed in the ^{13}C NMR spectra of the samples [29,30]. [b]From the intrinsic viscosities. [c] The melting temperatures were obtained with a differential scanning calorimeter Perkin Elmer DSC-7 performing scans in a flowing N_2 atmosphere and heating rate of 10°C/min [18]. [d] iamPP stands for isotactic amorphous polypropylene [31].

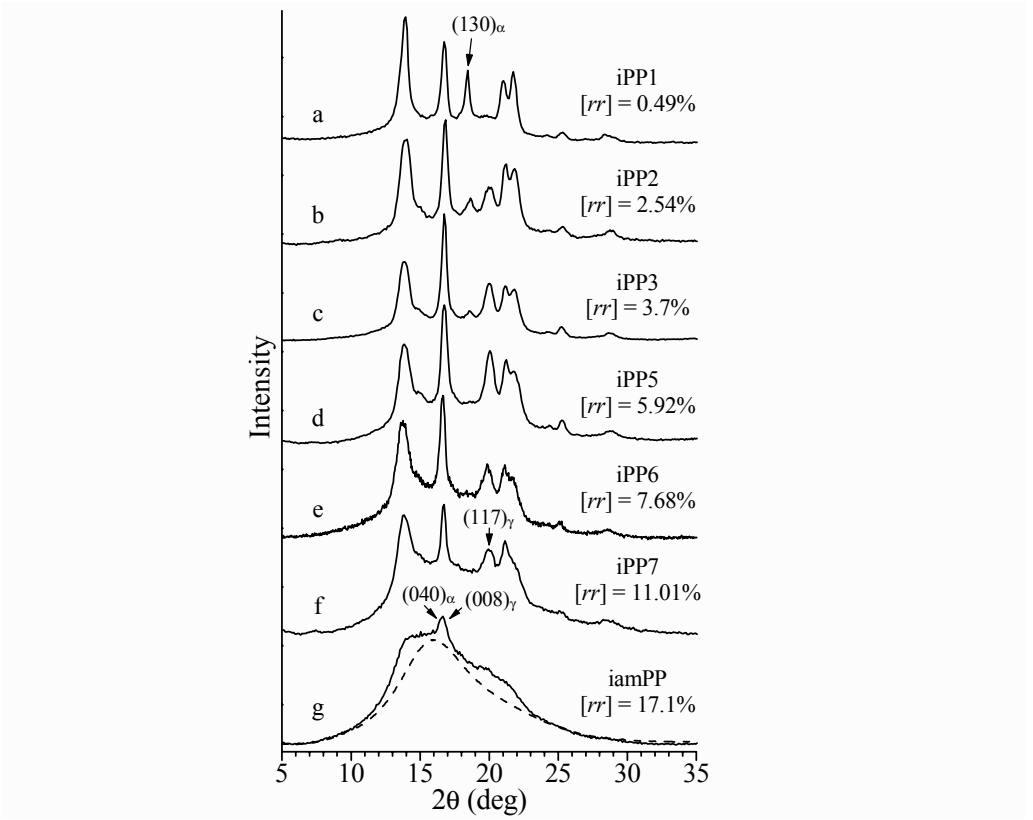

Fig. 17.2. X-ray powder diffraction profiles of iPP samples of Table 17.1 crystallized from the melt by compression molding and cooling the melt to room temperature at 1°C/min [18]. The *dashed line* indicates the diffraction profile of the amorphous phase. The $(130)_\alpha$ reflection of the α form [33] at $2\theta = 18.6°$ and the $(117)_\gamma$ reflections of the γ form [34] at $2\theta = 20.1°$ are indicated. The $(040)_\alpha$ and $(008)_\gamma$ reflections at $2\theta = 17°$ of α and γ forms, respectively, are also indicated

compression molded specimens of iPP samples of Table 17.1 are reported in Fig. 17.2. The samples iPP1-iPP7 crystallize from the melt as mixtures of α and γ forms (Fig. 17.3A and C, respectively), as indicated by the presence of both $(130)_\alpha$ and $(117)_\gamma$ reflections of α and γ forms, respectively, in the diffraction profiles of Fig. 17.2a-f. The intensity of the $(117)_\gamma$ reflection of the γ form at $2\theta = 20.1°$, increases with increasing concentration of *rr* defects [18].

The iPP sample of lowest stereoregularity (sample iamPP) does not crystallize by cooling the melt to room temperature, but slowly crystallizes in disordered modifications intermediate between α and γ forms (Fig. 17.3B), if the sample, cooled from the melt, is kept at room temperature for several days [32]. In fact, the X-ray diffraction profile of sample iamPP of Fig. 17.2g

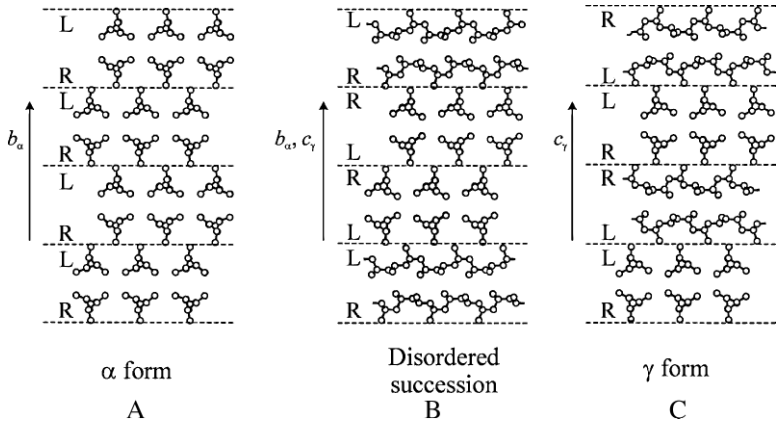

Fig. 17.3. Limit ordered models of packing proposed for α (A) and γ (C) forms of iPP and model of the α/γ disordered modifications intermediate between α and γ forms (B). The *dashed horizontal lines* delimit bilayers of chains. Subscripts α and γ identify unit cell parameters referred to the monoclinic [33] and orthorhombic [34] unit cells of α and γ forms, respectively. In the disordered model (B) consecutive bilayers of chains are stacked along b_α (c_γ) with the chain axes either parallel or nearly perpendicular, making α-like or γ-like arrangements of bilayers [32, 36]

presents only a sharp reflection at $2\theta = 17°$, corresponding to the $(040)_\alpha$ reflection of α form [33] or the $(008)_\gamma$ reflection of γ form [34]. The other sharp Bragg reflections of both α and γ forms, as $(110)_\alpha$ and $(130)_\alpha$ reflections at $2\theta = 14°$ and 18.6°, respectively, typical of the α form [33], and $(111)_\gamma$ and $(117)_\gamma$ reflections at $2\theta = 14$ and 20.1°, respectively, typical of the γ form [34] are absent. This indicates that the sample iamPP does not crystallize in the pure α or γ forms, but in a disordered modification intermediate between α and γ forms, [32, 35] containing disorder in the stacking along the b_α or c_γ direction of bilayers of chains with axes either parallel as in the α form or perpendicular as in the γ form (Fig. 17.3B) [35, 36].

The relative amount of γ form, with respect to the α-form in the melt crystallized samples of Fig. 17.2 is reported in Fig. 17.4 as a function of the concentration of *rr* defects. The most isotactic sample crystallizes basically in the α-form (Fig. 17.2a), with a limit low concentration of γ form of 15–20%. The amount of γ form increases with increasing content of *rr* defects up to 100% for *rr* concentrations higher than 6–7% [17, 18, 32].

The degree of crystallinity (Fig. 17.4) decreases only slightly with increasing concentration of *rr* defects in the range 0–11%, then drops to very low values for the less stereoregular sample iamPP.

The stress–strain curves of compression-molded films of iPP samples of Table 17.1 are shown in Fig. 17.5. The values of the most important mechanical parameters are reported in Fig. 17.6 as a function of the concentration of *rr* defects. The values of Young modulus decrease with increasing concentration

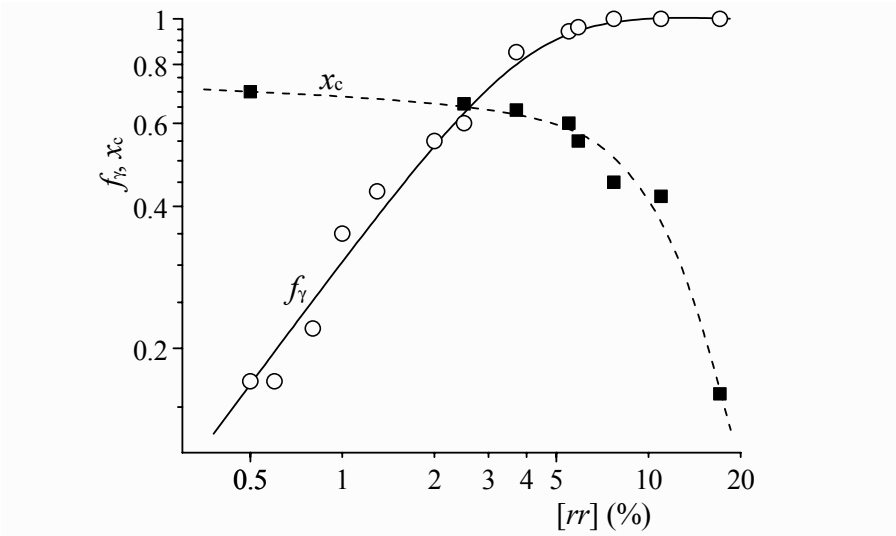

Fig. 17.4. Relative amount of γ form f_γ (◯), and degree of crystallinity x_c (■), in the iPP samples of Table 17.1 crystallized from the melt by compression molding and cooling the melt to room temperature at cooling rate of 1°C/min, as a function the concentration of *rr* defects [18]

of *rr* defects and decreasing crystallinity, from nearly 200 MPa of the sample iPP1 [18] to nearly 1 MPa of the poorly stereoregular sample iamPP [32] (Fig. 17.6A). The values of deformation at break, instead, increase with increasing concentration of defects (Fig. 17.6C). As expected, parallel to the decrease of the values of the modulus, a decrease of the stress at yielding with increasing concentration of defects is observed (Figure 17.6B) [18, 32].

Samples of iPP containing low concentration of *rr* defects (up to $[rr] = 3.7\%$, Figure 17.5A) show non uniform stretching behavior and high values of the elastic modulus (Fig. 17.6A) typical of stiff-plastic materials. Nevertheless, they present high ductility (Fig. 17.5A). In fact, these samples can be stretched at room temperature up to remarkable values of the strain (250–350%, Fig. 17.6C) [18].

A strong increase of the ductility and toughness is observed for higher contents of *rr* defects (Fig. 17.5B). In particular, samples with concentration of *rr* defects around 5–6% still present behavior of thermoplastic materials with slightly lower strength but much higher deformation at break ($\varepsilon_b \approx 1200\%$, Figs. 17.5B and 17.6C). This indicates that these samples ($[rr] = 5$–6% and melting temperatures around 110–115°C, for instance samples iPP4 and iPP5) behave as highly flexible thermoplastic materials [18].

The less crystalline samples, with concentration of *rr* defects in the range 7–11% (samples iPP6 and iPP7) show strong strain hardening at high deformation (Fig. 17.5B) with values of the tensile strength (32 MPa) higher than

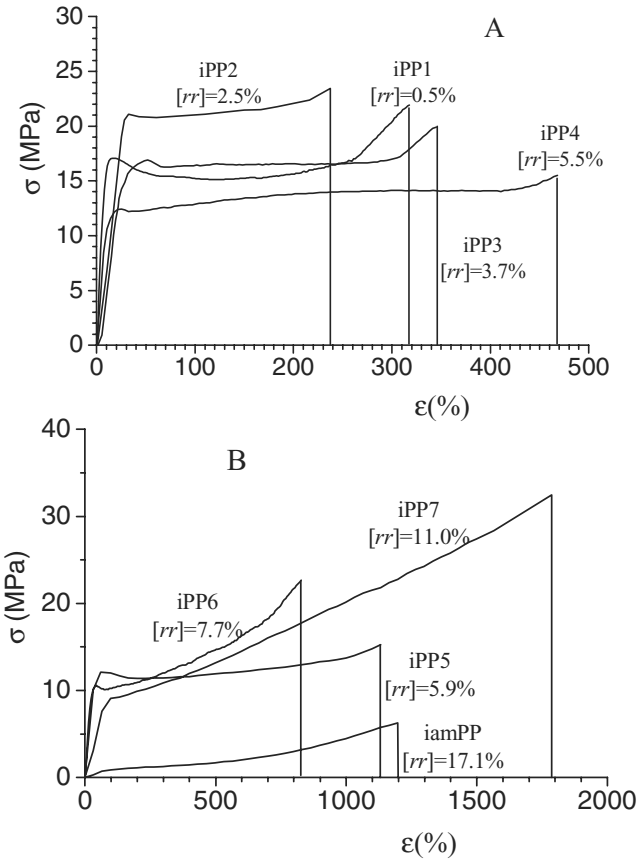

Fig. 17.5. Stress-strain curves of unoriented compression molded films of iPP samples of Table 17.1 [17, 18, 32]

those of the more isotactic and crystalline samples (20–23 MPa, Figures 17.5B and 17.6B) [18]. The strain hardening of these samples may be somehow related to the fact that they present uniform stretching behavior, crystals with low plastic resistance and therefore no cavitation [15]. Once crystals have experienced irreversible plastic deformations at low values of deformation, strain hardening is caused by straightening of the entangled network [15]. Similar strain hardening is experienced also by the lowest isotactic and crystalline sample iamPP [32], even though the achieved values of the tensile strength and the values of the stress at any strain are one order of magnitude lower than those of samples iPP6 and iPP7, because of the much lower level of crystallinity.

Samples with the highest concentration of *rr* defects ([*rr*] = 7–17%) show elastomeric properties. The stress-strain curves of samples iPP6, iPP7 and

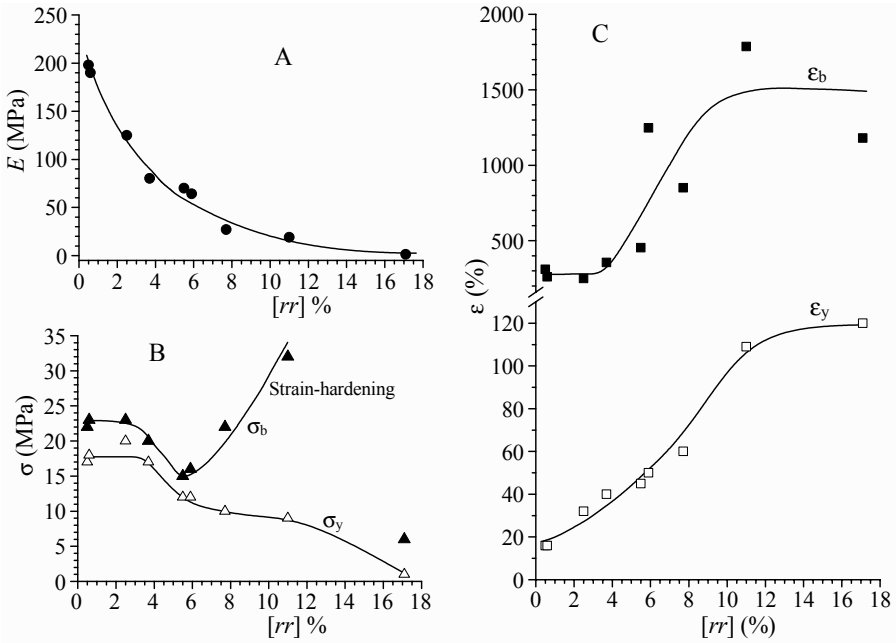

Fig. 17.6. Values of elastic modulus, E, (**A**), stress, σ, (**B**) and deformation, ε, (**C**) at break (*full symbols*) and at yield point (*open symbols*) as a function of concentration of *rr* defects of iPP samples of Table 17.1 [17, 18, 32]

iamPP present, indeed, typical shape of elastomeric materials (Fig. 17.5B), showing high values of deformation at break and strain-hardening at high deformations. The values of the tension set (t_s), that is the residual deformation achieved upon the release of the tension after stretching, measured at room temperature for unoriented films stretched up to the break or up to a deformation ε, are reported in Fig. 17.7. These values have been obtained as $t_s = 100(L_r - L_o)/L_o$, by stretching unoriented films of initial length L_0 up to the break, as in Fig. 17.5, or up to a deformation ε (final length L_f), then measuring the final length L_r of the relaxed sample ten minutes after breaking or after removing the tension. The low values of the tension set after breaking or after a deformation ε clearly indicate a good elastic behavior of the less stereoregular samples of Table 17.1 [18], especially of the sample iamPP [32].

In the samples iPP6 and iPP7, the elastic properties are associated with remarkable values of the modulus of nearly 20–30 MPa (Fig. 17.6A), and, as discussed before, very high values of tensile strength [18] (Fig. 17.6B). In the case of the poorly stereoregular sample iamPP, low values of the tension set are observed even at high deformation (Fig. 17.7), indicating that the sample iamPP experiences a recovery of the initial dimension after breaking as well as after removing the tension from any deformation [32]. The tension

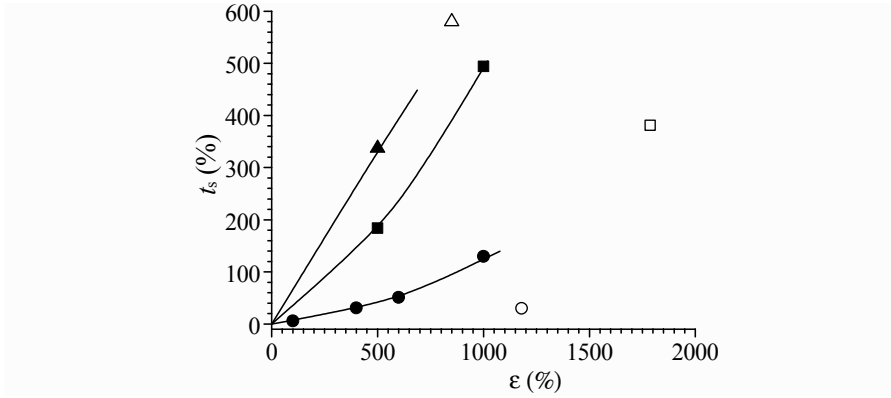

Fig. 17.7. Values of the tension set after breaking (*open symbols*), and after deformation ε (*full symbols*) of unoriented compression molded films of samples iPP6 (*triangles*), iPP7 (*squares*) [18], and iamPP (*circles*) [32].

set increases with increasing deformation, and values of tension set higher than those observed after breaking are obtained for the samples iPP7 and iamPP for values of deformation higher than 400%. This is probably due to the fact that the tension set after a given deformation ε has been measured after keeping the sample in tension for 10 min, allowing relaxation of the sample.

The elastic behavior of samples iPP6, iPP7 and iamPP is due to the fact that these samples are crystalline notwithstanding the low stereoregularity. These samples, indeed crystallize in the γ form of iPP or in α/γ disordered intermediate modifications thanks to the inclusion of most of the *rr* stereodefects (profiles e-g in Fig. 17.2) [18,32]. The formation of small crystalline domains induces elastomeric properties since crystals act as physical cross-links in the amorphous matrix, producing the elastomeric network. The presence of a high level of crystallinity (40–45%, Fig. 17.4) of samples iPP6 and iPP7, gives high values of the strength (Fig. 17.6), so that interesting thermoplastic elastomers with remarkable values of the modulus and tensile strength are obtained [17,18]. The small degree of crystallinity of the poorly stereoregular sample iamPP (∼16%), induces good elastic properties in a range of deformation larger than that shown by samples iPP6 and iPP7. The small crystalline domains that develops upon aging, act as physical knots of the elastomeric network, preventing the viscous flow of the amorphous chains and giving a typical thermoplastic elastomeric behavior. The poorly isotactic sample iamPP shows, indeed, poor elastic properties and viscous flow at high deformations in the amorphous state, before crystallization [32].

It has been argued that the outstanding mechanical properties of metallocene-made iPP samples containing only *rr* defects are related to the easy inclusion of *rr* defects inside the crystalline phase [17,18,32,36,37]. The high

ductility and good drawability at room temperature of these materials even when the concentration of *rr* defects is low and the samples basically crystallize in the α form, may be indeed explained by the fact that *rr* stereodefects are uniformly distributed between crystalline and amorphous phases, which have, therefore, the same composition. In these materials, the presence of defects in the crystals first of all decreases their plastic resistance. Moreover, the similar composition of the crystalline and amorphous phases makes the process of plastic deformation easier, reducing the stress level necessary for the destruction of the preexisting lamellae and re-crystallization of chains in new oriented crystallites with fibrillar morphology.

It is worth noting that metallocene-made iPP samples containing low amount of *rr* stereodefects (0.1–0.2%) and slightly higher concentration of defects of regioregularity (0.8–0.9% of 2,1 erythro units) are stiff and fragile with high values of the Young's modulus and very low values of deformation at break (ε_b around 6%) [37]. These samples do not undergo plastic deformation at room temperature and break before yielding. This behavior is similar to that of the commercial highly isotactic polypropylene prepared with Ziegler-Natta catalysts. It has been argued that the different effect of stereo- and regio-defects on the mechanical properties of iPP is probably related to their different levels of inclusion inside the crystalline phase. The amount of 2,1 regiodefects included in the crystalline phase, indeed, is much lower than that of *rr* stereodefects [38,39]. Since crystallization tends to reject the 2,1 regiodefects more strongly than the *rr* defects [35–37], in regioirregular iPP samples the composition of the crystalline and amorphous phases are not identical [37]. Therefore, regioirregular iPP samples are stiffer and more fragile than iPP samples containing only *rr* stereodefects, because the crystals show higher plastic resistance due to the low inclusion of regiodefects, and also because the non identical composition of the crystalline and amorphous phases makes the process of plastic deformation much harder, increasing the stress level necessary for the destruction of the crystalline lamellae up to values that produce breaking of the material [37].

17.3 Stress-induced Phase Transitions in Unoriented Fims

The plastic deformations of iPP samples of Table 17.1 are associated with irreversible morphological changes and polymorphic transitions. The structural and morphological transformations occurring during stretching of iPP samples of Table 17.1 have been analyzed by X-ray diffraction. Examples of X-ray fiber diffraction patterns are reported in Figs. 17.8–17.11 for samples having different concentration of *rr* defects.

The stretching behavior of unoriented films of the more stereoregular samples of Table 17.1 with *rr* content below 5%, is shown in Fig. 17.8, in the case of

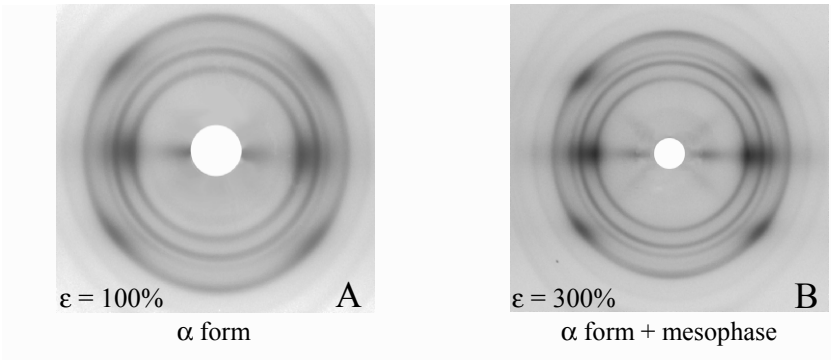

Fig. 17.8. X-ray fiber diffraction patterns of fibers of the sample iPP1 with $[rr]$ = 0.49% obtained by stretching at room temperature compression molded films at the indicated values of the strain ε [18]

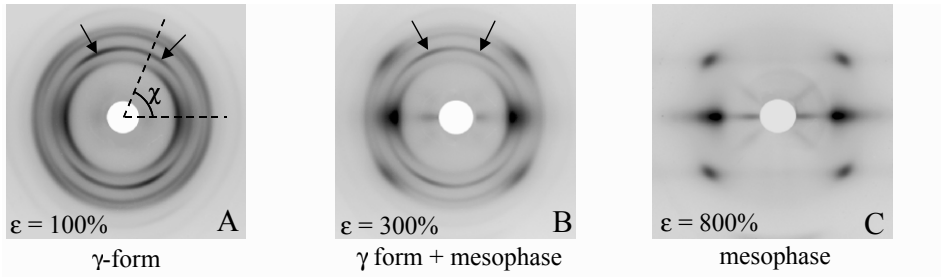

Fig. 17.9. X-ray fiber diffraction patterns of fibers of the sample iPP5 with content of rr defects of 5.9% obtained by stretching at room temperature compression molded films at the indicated values of the strain ε [18]

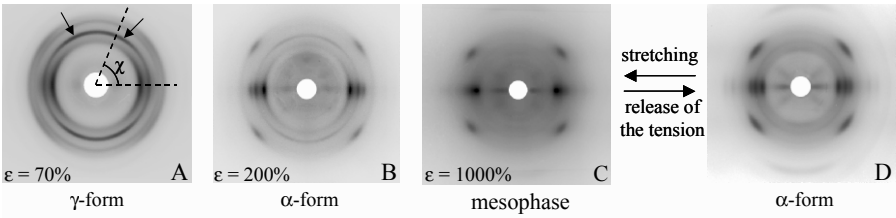

Fig. 17.10. X-ray fiber diffraction patterns of fibers of the sample iPP7 with content of rr defects of 11.01%, obtained by stretching compression molded films at the indicated values of the deformation ε keeping the fiber under tension (**A**–**C**) and after removing the tension from 1000% deformation (**D**) [18]

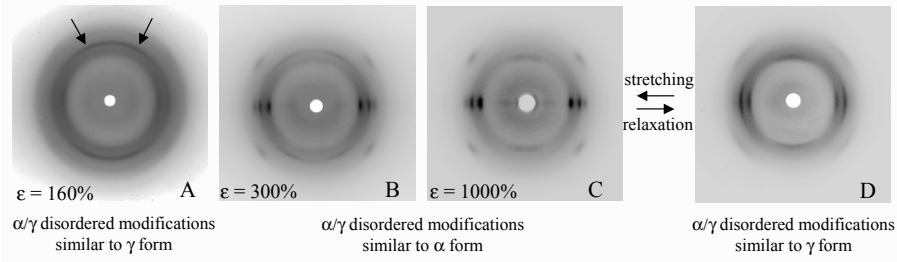

Fig. 17.11. X-ray fiber diffraction patterns (**A**–**C**) of fibers of the sample iamPP obtained by stretching at room temperature compression molded films at the indicated values of strain ε and after releasing the tension from 1000% deformation (**D**) [32]

the most isotactic sample iPP1 ($[rr] = 0.5\%$). For these samples, compression-molded unstretched films are generally crystallized in mixtures of α and γ forms (samples iPP2 and iPP3, Fig. 17.2b and c, respectively), whereas the sample iPP1 is basically in the α form (Fig. 17.2a) [18]. These samples behave as stiff plastic materials even though they can be easily stretched up to 200–300% deformation at room temperature (Fig. 17.5A). The crystalline form initially present in these samples partially transforms into the mesomorphic form already at low draw ratios (Fig. 17.8A) [18]. The formation of the mesomorphic form is indicated in the X-ray fiber diffraction pattern of the sample iPP1 stretched at 100% deformation, by the presence of a broad halo in the range of $2\theta = 14$–$18°$, typical of mesomorphic form of iPP, subtending non-oriented reflections of the α form (Fig. 17.8A). The stretching at room temperature of the most stereoregular iPP sample, does not produce high orientation of crystals, even at the maximum deformation before breaking (Fig. 17.8B), probably because of the limited possible deformation. A fraction of unoriented crystals of α form is still present even at the maximum possible deformation. Crystals that undergo plastic deformation and achieve orientation rapidly transform into the mesomorphic form, whereas non deformed crystals remains in the crystalline form (α form) of the initial unoriented film [18].

Samples with higher *rr* content, in the range 4–6%, are highly flexible materials that show very high deformation at break (Fig. 17.5A). For these samples, the γ form, originally present in compression-molded unstretched films (Fig. 17.2d), gradually transforms into the mesomorphic form by stretching. The gradual transformation of the γ form into the mesomorphic form at high draw ratios is shown in the case of sample iPP5 in Fig. 17.9, as an example [18].

Samples with concentration of *rr* defects in the range 7–11% are thermoplastic elastomers with high strength. For these samples, the γ form present in unstretched films (Fig. 17.2e,f) transforms by stretching into the α form, which, in turn, transforms into the mesomorphic form at very high defor-

mations, as shown as an example in Fig. 17.10 in the case of sample iPP7 ($[rr] = 11\%$) [18].

As discussed above, the poorly isotactic sample iamPP is essentially amorphous and does not crystallize from the melt due to the high concentration of defects. It slowly crystallizes upon aging at room temperature or by stretching in disordered modifications intermediate between the α and γ forms, with a maximum degree of crystallinity of only 16% (Fig. 17.2g) [32,35]. The stretching of this sample, even at high deformation, does not produce formation of the α form or the mesomorphic form, as instead occurs for the samples iPP6 and iPP7, but only α/γ disordered modifications, more similar to the α form are obtained (Fig. 17.11) [32,35]. This different behavior of the sample iamPP is due to the very short length of the regular isotactic sequences, the average value being only five monomeric units [35]. The observed crystallinity in this sample and in iPP samples having very low stereoregularity may be, indeed, explained by the fact that when the concentration of *rr* defects is high, these defects may be included in the crystals of γ form more easily than in the α form [35, 36]. More precisely, isolated *rr* triad defects can be easily tolerated at low cost of conformational and packing energy in the crystal lattices of α and γ forms of iPP and of the α/γ disordered modifications of Fig. 17.3B, but the inclusion in the γ form or in α/γ disordered modifications of Fig. 17.3B is more probable [32, 35, 36]. This explains the tendency of the sample iamPP to crystallize in disordered modifications intermediate between α and γ forms (Fig. 17.2g) and the fact that, for this sample, the pure α form is never obtained, even at high deformations [32, 35]. Disordered modifications intermediate between the α and γ forms more similar to the α form are instead obtained at high deformations (Fig. 17.11C), where a non-negligible fraction of bilayers of chains arranged with non parallel chain axes as in the γ form is still present [35].

The data of Fig. 17.9–17.11 indicate that the γ form of iPP is mechanically unstable, and tends to transform by stretching into the mesomorhic form in iPP samples with *rr* content in the range 2–6% [18] (Fig. 17.9), and into the α form (Fig. 17.10) or in disordered modifications intemediate between α and γ forms closer to the α form (Fig. 17.11), in less stereoregular iPP samples with *rr* content in the range 7–17% [17,18,32,35]. The transformation of γ form into modifications closer to the α form during stretching occurs through a continuum of disordered modifications intermediate between the α and γ forms [35]. More precisely, with increasing the draw ratio, the fraction of consecutive bilayers of chains faced with parallel chain axes as in the α-form increases, whereas the fraction of consecutive bilayers of chains faced with perpendicular chain axes as in the γ-form decreases (Fig. 17.3) [35]. This structural transformation is accompanied by the simultaneous increase of orientation of crystals with chain axes parallel to the stretching direction [32, 35].

It is worth noting that during the development of the fibrillar morphology, for deformations below a critical value that presumably coincide with

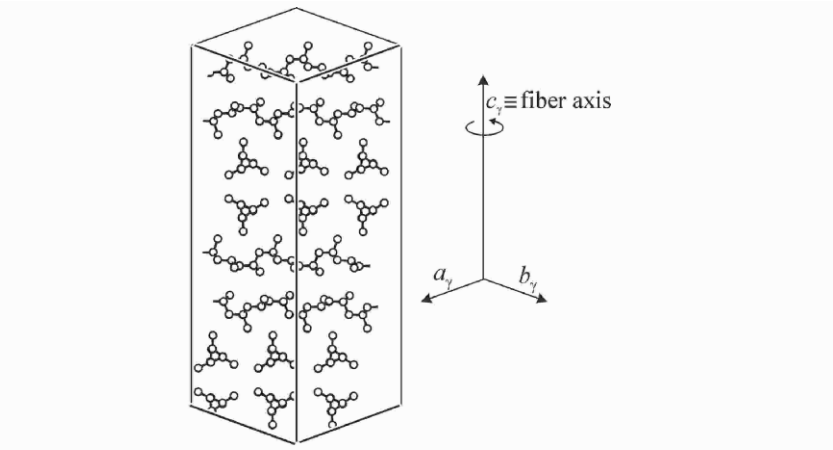

Fig. 17.12. Lamella of γ form oriented with the chain axes directed normal to the fiber axis and therefore with the c_γ axis, the piling direction of bilayers of chains, parallel to the z-axis (fiber axis, cross-β orientation)

the disappearance of γ form, changes of the texture of the sample also occur, consisting in the orientation of portion of the crystalline lamellae with the chain axes nearly perpendicular to the stretching direction instead than parallel, as in the standard fiber morphology (Fig. 17.12) [18, 32]. This non standard crystals orientation is achieved, for instance, in the case of the sample iPP5, iPP7 [18] and iamPP [32] up to values of deformation ε of 500, 400 and 600%, respectively, as indicated by the polarization of the $(040)_\alpha$ reflection of α form, or the $(008)_\gamma$ reflection of γ form at $d = 5.21$Å ($2\theta = 17°$), at oblique angles, indicated with arrows in Figures 17.9A,B, 17.10A and 17.11A. At higher deformations, the diffraction maxima at oblique angles disappear, and this reflection is polarized on the equator, as in the standard fiber morphology (Figs. 17.9C, 17.10C and 17.11C). The nearly meridional polarization of the reflection at $2\theta = 17°$ ($(008)_\gamma$ reflection of γ form or $(040)_\alpha$ reflection of α form) in the patterns of Fig. 17.9–17.11A indicates that portion of the crystals of γ form, or in disordered modifications intermediate between the α and γ forms more similar to the γ form, assume an orientation with the c_γ-axes of γ form (b_α axes of α form) nearly parallel to the stretching direction (Figure 17.12) [18,32]. Since the c_γ axes of γ form (b_α axes of α form) are the axes of stacking of bilayers of chains (Fig. 17.3) this non standard mode of orientation of iPP crystals corresponds to lamellae oriented with chain axes nearly perpendicular to the fiber axis (Fig. 17.12).

A similar kind of orientation has been well known for many years in some naturally occurring fibrous proteins such as silks [40]. The perpendicular orientation of chain axes with respect to the fiber axis, described as cross-β, occurs at low draw ratio and has been explained by the fact that in these soft

silks the small crystallites are elongated along the hydrogen bond directions, which run perpendicular to chain axes [40]. The cross-β orientation in iPP may be attributed to the simultaneous occurrence of two kinds of slip processes at low deformations, interlamellar and intralamellar [10]. Whereas interlamellar shear leads to a location of the $(008)_\gamma$ reflection of γ form ($(040)_\alpha$ reflection of α form) on the meridian, the intralamellar shear pushes the chain axes to align parallel with the stretching direction, and thus shifts the position of the reflection at $2\theta = 17^\circ$ toward the equator.

The fact that the cross-β orientation is apparent up to 500–600% deformation, indicates that not all the crystalline lamellae of γ form originally present in the sample experience simultaneously the uniaxial mechanical stress-field. The non standard mode of orientation of these crystals reflects crystallographic restraints on the slip processes, and topological constrains on the response of crystals to the tensile stress field. In the crystalline domains of γ form, indeed, the chains are oriented along two perpendicular directions, and the crystallites have the shape of elongated entities along the direction normal to the chain axes [18,32]. Because of the intrinsic structural and morphological characteristics of γ form, at low deformations portion of γ lamellae remains frozen in strained positions of the polymer matrix with the chain axes oriented nearly perpendicular to the stretching direction. By stretching at higher deformations the γ form transforms into the α form. Since in the crystals of α form the chains are all parallel, the deformation also induces orientation of crystals with the chain axes oriented along the stretching direction, as in a standard fiber morphology [18,32]. This mechanism is confirmed by the fact that this non standard mode of orientation of crystals has been observed only during stretching of iPP samples mainly crystallized in the γ form or in disordered modifications intermediate between the α and γ forms, and has never been observed for iPP samples crystallized in the pure α form.

The structural analysis of fibers of the iPP samples having different stereoregularity, have allowed building the phase diagram of iPP at room temperature reported in Fig. 17.13.

From the phase diagram the regions of stability of the different polymorphic forms of iPP in oriented fibers are defined as a function of stereoregularity and degree of deformation ε. The values of the critical strain at which the polymorphic transitions start and at which the transformation is complete depend on the stereoregularity. The critical values of the stress instead depend also on other parameters as, for instance, the degree of crystallinity of the sample, the amount of structural disorder present in the crystals and on the method of preparation of the test specimens.

It is apparent from Fig. 17.13 that for highly stereoregular iPP samples, with concentration of *rr* defects lower than 1% and content of isotactic pentad *mmmm* higher than 94%, the α form present in the unstretched melt-crystallized sample transforms into the mesomorphic form already at low deformations. For less stereoregular iPP samples, with content of *rr* defects in the range 2–6% and concentration of *mmmm* pentad in the range 68–94%,

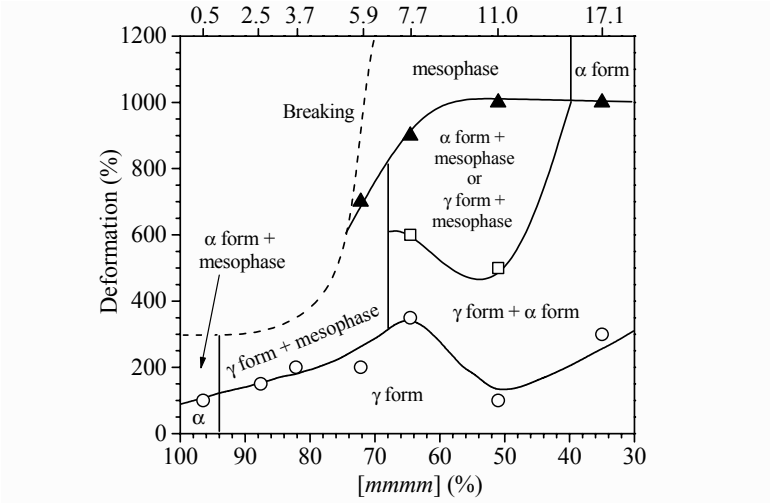

Fig. 17.13. Phase diagram of iPP showing the region of stability of the different polymorphic forms as a function of deformation ε ($\varepsilon = 100(L_f - L_0)/L_0$) and stereoregularity, defined as concentration of the fully isotactic pentads *mmmm*. The values of critical strains corresponding to the boundary lines between the various crystalline forms have been determined from the X-ray fiber diffraction patterns of Figs. 17.8–17.11. The concentration of *rr* triad defect is indicated in the *upper scale*. The deformation at break is also indicated (*dashed line*)

the unoriented melt-crystallized samples are in the γ form that transforms directly into the mesomorphic form by stretching at values of deformation higher than a critical value. For more stereoirregular samples, with *rr* content in the range 6–11% and concentration of *mmmm* pentad in the range 40–68%, the γ form transforms at low deformations into the α form which, in turn, transforms into the mesomorphic form with increasing deformation.

The transformation of α form into the mesomorphic form by stretching at values of deformation higher than a critical value has been already observed in the case of stretching at room temperature of iPP samples prepared with Ziegler–Natta catalysts [41]. These studies have indicated that there was no lamellar structure in the mesomorphic form of the iPP fibers. It has been suggested that the formation of the mesophase occurs through the destruction of the lamellar crystalline phase, probably by pulling chains out from crystals, and the dominant constituent of the mesomorphic form may be oriented bundles of helical chains [41]. Also for our metallocene-made iPP samples we can assume that the formation of the mesomorphic form, from fibers of α form, in the case of the elastomeric samples iPP6 and iPP7 (Fig. 17.10), or directly from the γ form in the case of the more stereoregular samples iPP2–iPP5, occurs via the pulling out of the chains from the lamellae of pre-existing crystalline form and successive re-organization of the chains in crystalline me-

somorphic aggregates. The latters are characterized by chains in 3/1 helical conformation, where the parallelism of the chain axes is maintained and only a poor correlation in the lateral positioning of the chain axes is present [42].

The transformation of γ form into the α form and/or into disordered modifications intermediate between the α and γ forms, closer to the α form, that occurs at low deformations in elastomeric stereoirregular iPP samples (with *rr* content higher than 7%, $[mmmm] < 60\%$), is also not direct. This transition is gradual, and occurs through a continuum of disordered modifications intermediate between the α- and γ-forms, and probably corresponds to the progressive breaking of the pre-existing lamellae with formation of the new ones during stretching. Direct transformation of γ form into α form is, in fact, prevented for steric reasons by the fact that whereas in the γ form the bilayers of chains are stacked along the c_γ-axis direction according to the sequence: [34] ...LRRLLR... (Fig. 17.3C, L and R standing for righ- and left-handed helical chains), in the α form the bilayers are stacked along the b_α-axis direction with a strict alternation of helical hands: [33] ...LRLRLR... (Fig. 17.3A). This transformation would imply simultaneous inversion of helical hand of the chains belonging to every bilayer, making a direct mechanism very unlikely.

It is worth noting that the presence of large biphasic regions in the phase diagram of Fig. 17.13 indicates that not all crystals undergo simultaneously phase transition during stretching, consistent with the fact that in semicrystalline polymers, whereas the strain is homogeneously distributed, the stress is not homogeneously distributed [3,6,14] and, at any strain only the crystals of a given form that experience a stress higher than a critical value undergo reorientation and/or transform into another polymorphic form. In other terms, the stress-induced phase transitions during plastic deformations are regulated by the same factors that govern the textural and morphological changes (transformations of spherultic morphology into fibrillar morphology and development of cross-β orientation of crystals), and reflects crystallographic restraints on the slip processes, and topological constraints on the response of crystals to the tensile stress field transmitted by the interconnected crystallites.

The above consideration support the hypothesis that when polymorphic transformations occur during plastic deformation, in iPP but also in many other polymers, the phase transitions are strain controlled rather than stress controlled [26]. As discussed above, the critical values of deformation at which the polymorphic transitions start always correspond to the destruction of the original lamellae of a given crystalline form, and re-crystallization with formation of fibrils in a new crystalline form. These critical values of the strain are indeed higher than the deformation values at point C of the stress-strain curve, that is the point at which the destruction of crystal blocks starts, followed by re-crystallization with formation of fibrils [3,10–13]. Moreover these critical values depend on the stereoregularity of the sample (Fig. 17.13). This suggests that the two factors that govern the location of the critical strain corresponding to the formation of fibrils, that is the modulus of the entangled amorphous and the stability of the crystal blocks [6], depend on the

stereoregularity. Chains of different stereoregularity possess, indeed, different flexibility. In fact, the relative configuration of consecutive stereoisomeric centers along the chain affects the space correlation among skeletal bonds and the rotational energy barriers around the C-C bonds [43]. Since the dynamics of macromolecular chains is largely controlled by these parameters, which can be defined as "the internal viscosity" [44], different degrees of stereoregularity produce a different entanglement density of the amorphous phase. The stereoregularity also affects the stability of crystals (besides the degree of crystallinity) and may influence the relative stability of the different polymorphic forms involved in the structural transformations [26]. In the case of iPP, it has been shown that the presence of *rr* defects induces crystallization from the melt of γ form and of disordered modifications intermediate between α and γ forms (Fig. 17.2), and affects the polymorphic transitions occurring during stretching of unoriented samples (Fig. 17.13). In particular, the easy inclusion of isolated *rr* triads defects in the crystal lattices of the α and γ forms of iPP [35,36], and the fact that when the concentration of *rr* defects is very high their inclusion in the γ form or in α/γ disordered modifications of Fig. 17.3B is more probable [37], explain the observed tendency of iPP samples of very low stereoregularity to crystallize achieving non negligible values of crystallinity. Moreover this also explains the fact that these samples crystallize in disordered modifications intermediate between α and γ forms [32,35], where the fraction of consecutive bilayers arranged as in the α-form increases with increasing deformation (Fig. 17.11 and 17.13).

17.4 Oriented Fibers of Elastomeric Samples

The analysis of the mechanical properties (Figs. 17.5–17.7) and the structural characterization of the stereoirregular elastomeric samples iPP6 and iPP7 have shown that, because of the presence of a significant level of crystallinity, unoriented films undergo irreversible plastic deformation that involves structural and morphological transformations. This explains the relatively high values of tension set measured after breaking or after a given deformation (Fig. 17.7), which indicate a non-complete elastic recovery after the first stretching [18]. In particular the more crystalline sample iPP6 presents an elastic recovery lower than that of the sample iPP7 (Fig. 17.7). Unoriented films of the less stereoregular sample iamPP, instead, show tension set values at any deformation and at break lower than those of samples iPP6 and iPP7, because of the lower degree of crystallinity [18,32].

For these samples a perfect elastic recovery is instead observed in successive cycles of stretching and relaxation of oriented fibers, regardless of stereoregularity [18, 32], as shown by the stress-strain hysteresis curves of fibers of samples iPP7 and iamPP reported in Fig. 17.14. These fibers have been prepared by stretching unoriented films obtained by compression molding up to 1000% and 600% deformation, for samples iPP7 and iamPP, re-

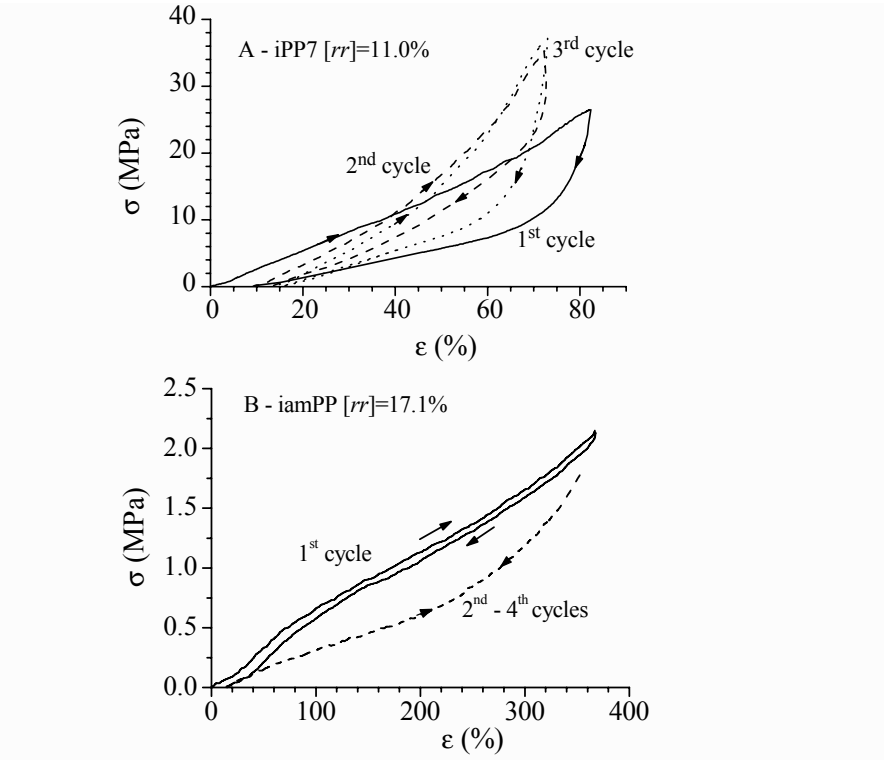

Fig. 17.14. Stress-strain hysteresis cycles recorded at room temperature, composed of stretching and relaxation (at controlled rate) steps according to the direction of the arrows, for stress-relaxed fibers of the samples iPP7 [17,18] (**A**) and iamPP [32] (**B**). The stress-relaxed fibers have been prepared by stretching compression-molded films, of initial length L_0, up to 1000% or 600% elongation, for the samples iPP7 and iamPP, respectively, (final lengths $L_f = 11L_0$ or $7L_0$, respectively), and, then, removing the tension. In the hysteresis cycles the stretching steps are performed stretching the fibers up to final length $L_f = 11L_0$ for the sample iPP7 and $L_f = 7L_0$ for the sample iamPP. (**A**) Continuous lines: first cycle; dashed lines: second cycle; dotted lines: third cycle and successive cycles. (**B**) Continuous lines: first cycle; dashed lines: curves averaged for at least four cycles successive to the first one

spectively, keeping the fibers under tension for 10 min at room temperature, then removing the tension, allowing the specimens to relax. The hysteresis cycles of Fig. 17.14 have been obtained by stretching the so prepared stress-relaxed oriented fibers, having the new initial length L_r, up to the final lengths $L_f = 11L_0$ and $7L_0$ for the samples iPP7 and iamPP, respectively, with L_0 the initial length of the unoriented film. It is apparent that successive hysteresis cycles, measured after the first one, are in all cases nearly coincident, indicating a tension set close to zero and a perfect elastic recovery [18,32].

Fibers of crystalline iPP6 and iPP7 samples show elastic behavior in a non trivial deformation range, which, however is much lower than the maximum deformation achieved during the preparation of the fibers [18]. This is due to the fact that unoriented films, when stretched at high deformation, do not experience total recovery of the initial dimension upon removing the tension (the tension set observed after the first stretching being higher than 100%, Fig. 17.7) [18]. Fibers of the less crystalline sample iamPP, instead, show elastic behavior in a much larger deformation range, nearly coincident with the maximum deformation achieved during the first stretching of unoriented films. In fact, since the unoriented films can be stretched up to very high deformation (up to 1200%) and experience a nearly total recovery of the initial dimension upon removing the tension (the tension set observed after the first stretching being very low even for large deformation, Fig. 17.7), the oriented fibers give elastic response in a large range of deformation, up to the maximum deformation achieved during the preparation of the fibers [32].

The stereoregularity also influences the polymorphic behavior of elastomeric iPP samples upon relaxation of fibers by releasing the tension. In the case of more isotactic and crystalline iPP6 and iPP7 samples, the mesomorphic form obtained by stretching at high draw ratios (Fig. 17.10C), transforms into the α form by releasing the tension (Fig. 17.10D) [18]. This transformation is reversible upon successive stretching and relaxing cycles and is associated with the fully elastic recovery of the sample (Figure 17.14A). The crystalline α form transforms by stretching into the disordered mesomorphic form, which, in turn, transforms back into the α form by releasing the tension (Fig. 17.10C and D) [18]. It is worth noting that the transformation of the disordered mesomorphic form into the α form corresponds to an increase of crystalline order. The crystallization upon removing the tension in stretched fibers is not common in polymers and is opposite to what is generally observed in a common elastomer as the natural rubber, for which crystallization occurs during stretching, whereas melting occurs upon releasing the tension [45, 46]. The crystallization of the mesomorphic form into the α form upon releasing the tension is not observed in the case of flexible or stiff-plastic samples (Figs. 17.8 and 17.9), which do not show elastic behavior. This indicates that in the elastomeric samples elasticity is probably partially due to the enthalpic contribution associated with the crystallization of the mesomorphic form into the α form [18].

Also in the case of the poorly isotactic sample iamPP the elastic recovery observed upon releasing the tension (Fig. 17.14B) is associated with a polymorphic transformation occurring inside the crystalline domains. Disordered α/γ modifications of iPP very close to the α form, having a high fraction of consecutive bilayers facing as in the α form with parallel chain axes, formed during stretching (Fig. 17.11C), transform back into more disordered modifications closer to the γ form upon releasing the tension (Fig. 17.11D), with a simultaneous decrease of the degree of orientation of the crystals [32]. These small crystalline domains act as physical knots in an amorphous matrix. The

chains belonging to the amorphous phase, connecting the crystalline regions, undergo a reversible conformational transition between the entropically favored disordered random coil conformation in the unstretched state and the extended conformation in the stretched state. Therefore, the entropic effect due to this conformational transition is responsible for the elasticity. These amorphous chains are entangled and connect, as tie-chains, the small crystalline domains. They act as springs between the crystals being well-oriented and in extended conformation in the stretched state and return in the disordered coil conformation when the tension is removed [32].

It is worth noting that after the first hysteresis cycle, whereas in the case of elastomeric samples iPP6 and iPP7 a remarkable increase of the strength occurs (Fig. 17.14A) (hardening), in the case of the sample iamPP the stress at any strain decreases (Fig. 17.14B) (softening). The hardening in the case of more crystalline elastomeric samples iPP6 and iPP7 maybe, somehow, related to the increase of crystallinity and the structural transitions occurring during stretching. The formation of the metastable mesomorphic form at high deformation and the successive crystallization into the α form upon relaxation may play an important role. In the case of the sample iamPP instead, softening may be somehow related to a decrease of entanglement density due to viscous flow of amorphous chains.

17.5 Conclusions

The non trivial role of crystalline phase during plastic deformation has been examined in the case of samples of isotactic polypropylene prepared with metallocene catalysts. Samples with high molecular mass and variable stereoregularity, containing only *rr* stereo-defects and no regio-defects, have been analyzed. These samples show crystallization and mechanical properties that depend on the degree of stereoregularity. The continuous change of mechanical properties of metallocene-made iPP samples as a function of concentration of *rr* defects of stereoregularity is shown in Fig. 17.15. Samples with low concentration of *rr* defects, up to 3–4%, present high melting temperatures, in the range 162–130°C, and behave as stiff plastic materials. Sample with higher *rr* content, in the range 4–6%, and melting temperatures around 115–120°C are highly flexible thermoplastic materials, showing very high deformation at break. Samples with concentration of *rr* defects in the range 7–11% and melting temperature in the range 80–110°C are thermoplastic elastomers with high strength. Samples with concentration of *rr* defects higher than 11% and melting temperature lower than 50°C are soft materials with elastomeric properties more similar to those of conventional thermoplastic elastomers.

The samples show a complex polymorphism during tensile deformation. The relationships between the different mechanical behavior and the stress-induced phase transitions are discussed in terms of a general view, outlining the concept that stress-induced phase transitions during plastic deformation of

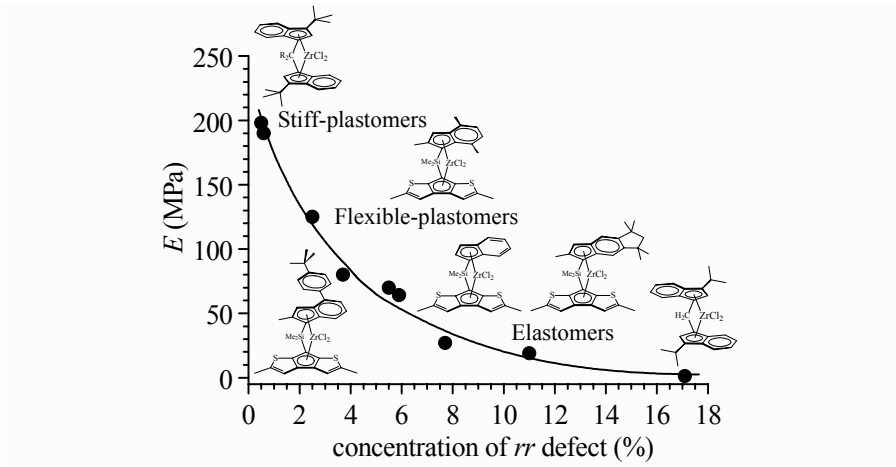

Fig. 17.15. Classification of i-PP samples prepared with different catalysts, as stiff-plastic materials, flexible-plastic materials, and thermoplastic elastomers depending on concentration of *rr* defects of stereoregularity and Young's modulus (E)

semicrystalline polymers are governed by the same rules that govern their deformation behavior. Polymorphic transformations occur through breaking of preexisting lamellae of the original crystalline form and formation of fibrils of the new crystalline form. These transitions, for a given sample, appear strain controlled rather than stress controlled. The values of the critical strain linked to the polymorphic transitions are namely affected by the chain microstructure, whereas the corresponding values of the stress depend on the degree of crystallinity, the amount of structural disorder present in the crystals and on the relative stability of the two involved crystalline forms. A phase diagram of iPP where the regions of stability of the different polymorphic forms are defined as a function of stereoregularity and degree of deformation has been built.

Stress-induced phase transitions may play a key role also in determining elastic properties in polymeric materials. In fact semicrystalline polymers generally show only short-range elasticity when stretched samples are relaxed by releasing the tensile stress. Long range elasticity, when present, is, instead, generally associated with the occurrence of polymorphic transitions. In the case of elastomeric iPP, we have shown that samples of different stereoregularity present different types of elasticity depending on the degree of crystallinity. The more stereoregular samples, with *rr* content in the range 7–11% show elastic behavior in spite of the high degree of crystallinity (40–50%). Since elasticity is generally a property of the amorphous phase, probably elasticity in these samples is partially due to the enthalpic contribution associated with the crystallization of the mesomorphic form into the α form occurring upon

releasing the tension. In the case of the poorly stereoregular sample iamPP, instead, the degree of crystallinity is low, and elasticity has essentially entropic origin as in conventional elastomers.

Acknowledgment

Financial supports from Basell Ferrara, Italy and from the "Ministero dell' Istruzione, dell'Università e della Ricerca" (PRIN 2004) are gratefully acknowledged. We thank Dr. Luigi Resconi of Basell for providing the polymer samples and for having stimulated this study.

References

[1] Flory, P. J.; Yoon, D. Y. *Nature (London)* **1978**, 272, 226.
[2] Peterlin, A. *J. Mater. Sci.* **1971**, 6, 490.
[3] Galeski, A. *Progr. Polym. Sci.* **2003**, 28, 1643.
[4] Argon A. S.; Cohen, R. E. *Polymer* **2003**, 44, 6013.
[5] Oleinik, E. F. *Polymer Sci. Ser. C.* **2003**, 45, 17.
[6] Men, Y.; Rieger, J.; Strobl, G. *Phys. Rev. Lett.* **2003**, 91, 95502.
[7] Hughes, D. J.; Mahendrasingam, A.; Oatway, W. B.; Heeley, E. L.; Martin, C.; Fuller, W. *Polymer* **1997,** 38, 6427; Yamada, M.; Miyasaka, K.; Ishikawa, K. *J. Polym. Sci.* **1971**, *A*29, 1083; Takahashi, Y.; Ishida T. *J. Polym. Sci., Polym. Phys.* **1988**, 26, 2267.
[8] Liu, Y.; Kennard, C. H. L.; Truss R. W.; Carlos, N. J. *Polymer* **1997**, 38, 2797.
[9] Ferreiro, V.; Coulon, G. *J. Polym. Sci., Polym. Phys.* **2004**, 42, 687.
[10] (a) Hiss, R.; Hobeika, S.; Lynn, C.; Strobl, G. *Macromolecules* **1999**, 32, 4390; (b) Men Y.; Strobl, G. *J. Macromol. Sci. Physics* **2001**, *B*40, 775.
[11] Al-Hussein, M.; Strobl, G. *Macromolecules* **2002**, 35, 8515.
[12] Men Y.; Strobl, G. *Macromolecules* **2003**, 36, 1889.
[13] Hobeika, S.; Men Y.; Strobl, G. *Macromolecules* **2000**, 33, 1827.
[14] Hong, K.; Rastogi, A.; Strobl, G. *Macromolecules* **2004**, 37, 10165; *Macromolecules* **2004**, 37, 10174.
[15] Pawlak, A.; Galeski, A. *Macromolecules* **2005**, 38, 9688.
[16] Auriemma, F.; De Rosa C.; Corradini, P. *Adv. Polym. Sci.* **2005**, 181, 1.
[17] De Rosa, C.; Auriemma, F.; Di Capua, A.; Resconi, L.; Guidotti, S.; Camurati, I.; Nifant'ev, I. E.; Laishevtsev, I. P. *J. Am. Chem. Soc.* **2004**, 126, 17040.
[18] De Rosa, C.; Auriemma, F.; De Lucia, G.; Resconi, L. *Polymer* **2005**, 46, 9461.
[19] Auriemma, F.; Ruiz de Ballesteros, O.; De Rosa, C. *Macromolecules* **2001**, 34, 4485.
[20] Auriemma, F.; De Rosa, C. *J. Am. Chem. Soc.* **2003**, 125, 13143.
[21] F. Auriemma and C. De Rosa, *Macromolecules* **2003**, 36, 9396.
[22] Ewen, J. A.; Elder, M. J.; Jones, R. L.; Haspeslagh, L.; Atwood, J. L.; Bott, S. G.; Robinson, K. *Makromol. Chem. Macromol. Symp.* **1991**, 48/49, 253.
[23] Brintzinger, H.H.; Fisher, D.; Mulhaupt, R.; Rieger, B.; Waymouth, R. M. *Angew. Chem. Int. Ed. Engl.* **1995**, 34, 1143.
[24] Kaminsky, W. *Macromol. Chem. Phys.* **1996**, 197, 3907.

[25] Resconi, L.; Cavallo, L.; Fait, A.; Piemontesi, F. *Chem. Rev.* **2000**, 100, 1253.
[26] De Rosa, C.; Auriemma, F.; Ruiz de Ballesteros, O. *Phys. Rev. Lett.* **2006**, 96, 167801.
[27] Nifant'ev, I.E.; Guidotti, S.; Resconi, L.; Laishevtsev, I.. PCT Int Appl WO 01/47939. Basell, Italy; 2001.
[28] Resconi, L.; Guidotti, S.; Camerati, I.; Nifant'ev, I.E.; Laishevtsev, I. *Polym. Mater. Sci. Eng.* **2002**, 87, 76.
[29] Fritze, C.; Resconi, L.; Sculte, J.; Guidotti, S. PCT Int Appl WO 03/00706. Basell, Italy; 2003.
[30] Nifant'ev, I. E.; Laishevtsev, I. P.; Ivchenko, P. V.; Kashulin, I. A.; Guidotti, S.; Piemontesi, F.; Camurati, I.; Resconi, L.; Klusener, P. A. A.; Rijsemus, J. J. H.; de Kloe, K. P.; Korndorffer, F. M. *Macromol. Chem. Phys.* **2004**, 205, 2275. Resconi, L.; Guidotti, S.; Camurati, I.; Frabetti, R.; Focante, F.; Nifant'ev, I. E.; Laishevtsev, I. P. *Macromol. Chem. Phys.* **2005**, 206, 1405.
[31] Balboni, D.; Moscardi, G.; Baruzzi, G.; Braga, V.; Camurati, I.; Piemontesi, F.; Resconi, L.; Nifant'ev, I. E.; Venditto, V.; Antinucci, S. *Macromol. Chem. Phys.* **2001**, 202, 2010.
[32] De Rosa, C.; Auriemma, F.; Perretta, C. *Macromolecules* **2004**, 37, 6843.
[33] Natta, G.; Corradini, P. *Nuovo Cimento* **1960**, 15, 40–51.
[34] Bruckner, S.; Meille, S. V. *Nature* **1989**, 340, 455–457.
[35] Auriemma, F.; De Rosa, C.; Boscato, T.; Corradini, P. *Macromolecules* **2001**, 34, 4815.
[36] Auriemma F.; De Rosa C. *Macromolecules* **2002**, 35, 9057.
[37] De Rosa, C.; Auriemma, F.; Paolillo, M.; Resconi, L.; Camurati, I. *Macromolecules* **2005**, 38, 9143.
[38] VanderHart, D. L.; Alamo, R. G.; Nyden, M. R.; Kim, M. H.; Mandelkern, L. *Macromolecules* **2000**, 33, 6078.
[39] Nyden, M. R.; VanderHart, D. L.; Alamo, R. G. *Comput. Theor. Polym. Sci.* **2001**, 11, 175.
[40] Geddes, A. J.; Parker, K. D.; Atkins, E. D. T.; Beighton, E. *J. Mol. Biol.* **1968**, 32, 343.
[41] Ran, S.; Zong, X.; Fang, D.; Hsiao, B. S.; Chu, B.; Phillips, R.A.; *Macromolecules* **2001**, 34, 2569.
[42] Corradini, P.; Petraccone, V.; De Rosa, C.; Guerra, G. *Macromolecules* **1986**, 19, 2699. Corradini, P.; De Rosa, C.; Guerra, G.; Petraccone, V. *Polymer Commun.* **1989**, 30, 281.
[43] Flory, P. J *Statistical Mechanics of Chain Molecules* John Wiley &Sons, New York: 1969.
[44] Allegra, G. *J. Chem. Phys.* **1974**, 61, 4910.
[45] Treolar, L. R. G. The physics of rubber elasticity. Oxford: Claderon Press; 1975.
[46] Tosaka, M.; Murakami, S.; Poompradub, S.; Kohjiya, S.; Ikeda, Y.; Toki, S.; Sics, I.; Hsiao, B. *Macromolecules* **2004**, 37, 3299.